Characterization of a Potential New Half-Metallic Ferromagnet: $Yb_{14}MnSb_{11}$

A. P. Holm,[1] S. M. Kauzlarich,[1] S. A. Morton,[2] G. D. Waddill,[2] W. E. Pickett,[3] and J. G. Tobin[4]

[1]*Department of Chemistry, University of California, One Shields Ave., Davis, CA 95616*
[2]*Department of Physics, University of Missouri-Rolla, Rolla, MO 65401-0249*
[3]*Department of Physics, University of California, One Shields Ave., Davis, CA 95616*
[4]*Lawrence Livermore National Laboratory, Livermore, CA 94550*

X-ray magnetic circular dichroism measurements (XMCD) indicate full, perfect spin alignment in the Mn (five aligned spins) and suggest that $Yb_{14}MnSb_{11}$ is a half-metallic ferromagnet. The compound is isostructural to $Ca_{14}AlSb_{11}$, with the Mn occupying the Al site in the $[AlSb_4]^{9-}$ discrete tetrahedral, anionic unit. Bulk magnetization measurements exhibit a saturation moment of $3.90 \pm 0.02\ \mu_B$/ formula unit consistent with 4 unpaired spins and implying a Mn^{3+}, high spin d^4 state. XMCD measurements reveal that the Mn L_{23} is strongly dichroic, the Sb M_{45} shows a weak dichroism that is antialigned to the Mn, and the Yb N_{45} shows no dichroism. Comparisons of the Mn spectra with the theoretical models for Mn^{2+} show excellent agreement. The bulk magnetization can be understood as full spin alignment (five spins up) of the Mn^{2+} with cancellation of one spin by an antialigned moment from the Sb 5p band of the Sb_4 cage surrounding the Mn.

I. INTRODUCTION

The recent commercial development of spin-polarized electronic transport devices for use in magnetic information storage has initiated great interest in developing new materials possessing unique magnetic and electronic properties for direct applications in magnetoelectronic devices.[1] This phenomenon has spurred great interest in developing conducting materials that possess 100% spin-polarization at the Fermi level, a class of materials that de Groot *et al.* first termed half-metallic ferromagnets (HMFM).[2] The primary candidates for study are ternary intermetallic compounds including the spinels, such as Fe_3O_4,[3] the various Heusler phases, such as Mn_2Val,[4] and the half-Heusler alloys, most notably NiMnSb and PtMnSb.[2, 5-7] Compounds with the perovskite structure, $La_{0.7}Ca_{0.3}MnO_3$,[8] and $La_{0.7}Sr_{0.3}MnO_3$,[9] and the double perovskite structure, Sr_2FeMoO_6,[10, 11] are also strong candidates for half-metallicity. In addition, much simpler binary compounds such as CrO_2 are also suggested as half-metals[12-15] All of these compounds share a sufficient amount of complexity in both their electronic and crystal structures to encourage gaps in the spin specific density of states which is a requirement for half-metallicity.[16]

Recently, Pickett and Singh proposed a correlation between half-metallicity and colossal magnetoresistance (CMR) in a study of the perovskite CMR material $La_{1-x}Ca_xMnO_3$.[8] Half-metallicity has been experimentally indicated through the use of spin-resolving photoemission of the related perovskite CMR material, $La_{0.7}Sr_{0.3}MnO_3$.[9] The proposal that the CMR effect could be closely associated with, or resulting from a half-metallic nature has made the CMR compound, $Yb_{14}MnSb_{11}$, a candidate HMFM. In addition, the significant degree of complexity in the compound's unique electronic and

crystal structures supports $Yb_{14}MnSb_{11}$'s candidacy for half-metallicity. The compound, $Yb_{14}MnSb_{11}$, belongs to a particular class of materials termed transition metal Zintl phases,[17-40] and offers a distinct opportunity to study interesting magnetic phenomena due to the combination of an intricate crystal structure, an apparent Mn-only saturation moment of 3.90 ± 0.02 μ_B/ formula unit, and the CMR effect. In this paper, we take advantage of the elemental specificity allowed in X-ray magnetic circular dichroism (XMCD) to probe the specific nature of the magnetic moment on Mn and Sb. Our XMCD results clearly indicate a large dichroism signal within the Mn L_{23} edges due to a large magnetic moment present on the Mn, a small antialigned moment on Sb as revealed in the Sb M_{45}, and no moment on Yb as observed in the Yb N_{45}. When coupled with the bulk magnetization value of ~4 μ_B/ formula unit, these results demonstrate that full alignment of the unpaired Mn spins is achieved, and there is a small moment on Sb that is antialigned with the Mn moment. Since $Yb_{14}MnSb_{11}$ is closely related to the $Ca_{14}MnBi_{11}$ and $Ba_{14}MnBi_{11}$ compounds whose electronic structure is nearly half-metallic when ferromagnetically aligned, our results are consistent with $Yb_{14}MnSb_{11}$ being a half-metallic ferromagnet or very close to it. The XMCD results will be discussed in light of the bulk magnetic measurements here.

II. EXPERIMENTAL

Single crystal samples of $Yb_{14}MnSb_{11}$ were grown by a high temperature molten metal flux as described elsewhere.[24, 41] Full magnetic and transport measurements have been published.[19, 24, 41] The crystals used in this experiment were characterized by single

crystal magnetic susceptibility. DC magnetization data were obtained with a Quantum Design MPMS Superconducting Quantum Interference Device (SQUID) magnetometer with a 7 Tesla superconducting magnet. Data were collected and analyzed with the Magnetic Property Measurement System (MPMS) software provided. The crystal was placed in a gel capsule and suspended in a straw. The orientation was determined by a series of magnetization vs. field measurements and aligned according to the easy magnetization axis (*c*-axis). Magnetization vs. temperature data were obtained and a Curie temperature (T_C) of ~53 Kelvin was measured, consistent with previously published results.[19, 24] The crystals were measured before and after the XMCD measurements to verify the integrity of the samples. The XMCD experiments of Mn L_{23}, Sb M_{45}, and Yb N_{45} were performed using the elliptically polarized undulator (EPU) of Beamline 4.0 at the Advanced Light Source.[42-44] The spectra were measured using the total photoelectron yield method by detecting the sample current as a function of photon energy through the absorption edge. Examples of the absorption spectra are shown in Figure 2. The base chamber pressure was maintained at better than 1×10^{-9} torr throughout the experiments. Single crystal samples of $Yb_{14}MnSb_{11}$ were mounted on a copper sample stage fit with permanent magnets of Ni-coated NdFeB alloy rated at a magnetic field of 4000 G. Taking advantage of the anisotropic magnetization, samples were oriented with the magnetically easy axis (*c*-axis) along the Poynting vector. The sample stage was cooled to and maintained at a temperature of 20K throughout the experiments. Clean surfaces were obtained by cleaving the samples *in situ* with a two-blade cleaving tool and comparing the resulting left and right polarized Mn L_{23} XAS spectra to the same for the uncut spectra.

III. DISCUSSION

The $Yb_{14}MnSb_{11}$ compound is isostructural to $Ca_{14}AlSb_{11}$, and its structure shown in Figure 1 can be described as containing 14 Yb^{2+} cations, an $[MnSb_4]^{9-}$ tetrahedron, an $[Sb_3]^{7-}$ polyatomic anion, and 4 Sb^{3-} isolated anions. The tetrahedra are surrounded by a cage of Yb^{2+} cations, and stack in an alternating pattern with the Sb linear anions along the *c*-axis giving an effective Mn···Mn distance of 10 Å between each tetrahedron. The DC magnetization data at 20 Kelvin and 5 Kelvin (inset) are presented in Figure 2 for a single crystal of $Yb_{14}MnSb_{11}$ aligned along the easy magnetization axis (*c*-axis). The observed saturation moment of 3.90 ± 0.02 μ_B/ formula unit is seemingly consistent with the value of 4 μ_B/ Mn assigned to four unpaired electrons on an Mn^{3+} ion. This interpretation is the simplest that provides an overall accounting of charge for the $[MnSb_4]^{9-}$ anion and the additional structural components. However, things are not as simple as they seem to be. XMCD measurements were carried out in order to gain a better understanding of the ferromagnetic and magnetoresistive behavior observed in this compound. The advantage in using this technique is the ability to specifically probe each element of the system, and quantitatively assign the magnetic contribution of each constituent to the total magnetic moment. Because of this element specificity, a quantitative assignment of the source of the bulk magnetization measured in the DC magnetization experiments can be given to the present system. Measurements of the Mn L_{23}, Sb M_{45}, and Yb N_{45} absorption edges for both +0.9 and –0.9 helicity along with the *M*(*H*) data are given in Figure 2. A significant dichroism is apparent in the Mn edge and

is consistent with the magnetic ordering that arises from the Mn component of the system. In addition, the Sb M_{45} indicates a small difference that is antiferromagnetically aligned to Mn. Finally, the Yb N_{45} spectrum demonstrates no dichroism and is consistent with a nonmagnetic assignment due to a closed shell Yb(2+) configuration. The observation of a single peak for the Yb 4d doublet is consistent with previous observations.[45]

A comparison of the experimental dichroic difference with atomic calculations of the magnetically ordered Mn^{2+} in Figure 3a display good agreement.[46] The calculated spectrum is convoluted with an energy dependent gaussian function to account for experimental lifetime broadening effects. This type of comparison was chosen over a direct calculation of the magnetic moment using a sum rules approach due to the inability for sum rules to accurately account for the multi-electronic effects possibly present on the Mn, and also the inability to account for the crystal field effects that influence this system.[47, 48] The atomic calculations of van der Laan and Thole provide these necessary requirements with the ability to make comparisons between various crystal fields and oxidation states. By comparison of our experimental XMCD spectrum with those calculated for Mn^{2+} and Mn^{3+} in crystal field symmetry, we have concluded that the best agreement is with the calculated XMCD spectrum for Mn^{2+}. These results are further supported by the extremely poor agreement found between the calculated spectrum for the Mn^{3+} ion and the experimental data. The correct valence assignment for the Mn ion is 2+ which does not appear to be consistent with the bulk magnetization data and contradicts the valence assignments and charge balance previously given.[18-21, 24, 27, 30-32, 34, 35, 37-39, 49] However, a recent theoretical study of the bonding, moment formation and

magnetic interactions of the related $Ca_{14}MnBi_{11}$ and $Ba_{14}MnBi_{11}$ systems suggests a new model to account for the discrepancy between electron counting and the experimental data.[16] Using an efficient, local orbital based method within the local spin density approximation, they find that Mn is high-spin d^5 and the bonding bands lack one electron per formula unit of being filled. Even though this arrangement would leave the Mn 3d states fully occupied, the ~4μ_B/ formula unit experimental magnetic moment would be maintained due to a hole in the Pn_4 tetrahedron aligning parallel to the Mn moment, and the unpaired electron associated with the hole aligning antiparallel to the Mn moment. The XMCD spectrum for Sb M_{45} (Figure 3b) shows a small dichroism effect that indicates anti-alignment of the moment on Sb with the moment on Mn, confirming the prediction of a hole on the Pn valence *p* states of the tetrahedron lying parallel to the moment on the Mn. Note the sign reversal of the dichroism between Figures 3a and 3b. Thus, the element specific measurements furnished by XMCD and the explanation of the spectral behavior offered by theory are in excellent agreement with the bulk magnetization data.

These findings show complete polarization of the Mn spins as indicated by the bulk magnetization measurement, theory, the Mn dichroism in XMCD and the antiferromagnetic ordering observed in the small moment of Sb, also by XMCD. This result itself is important in that a perfect Mn^{2+}, 5μ_B moment has been directly observed. This seeming violation of the Slater-Pauling curve can only occur because the Mn exists in an Yb-Sb matrix which separates yet permits communication between Mn ions.[50] Other similar systems have exhibited large Mn moments, but none as large as 5μ_B.[51-53] The most important criterion for a half-metallic ferromagnet is 100% polarization of

spins at the Fermi energy for a metallic system. The compound, $Yb_{14}MnSb_{11}$, is a poor metal that we have shown to possess 100% polarization of spins in the Mn (five aligned spins) and only $4\mu_B$/ formula unit as indicated by a bulk saturation magnetization moment that is consistent with four unpaired spins on the Mn^{2+} ion. The fifth unpaired electron in Mn is anti-aligned to and cancelled by an unpaired electron on the Sb 5*p* states of the tetrahedron, as indicated in Figure 3b by the XMCD for Sb M_{45}. It seems likely, based upon the oxidation state of the Yb^{2+} and the semiconducting nature of Sb, that neither Yb nor Sb has conducting electrons at the Fermi energy. For example, the fourteen 4*f* electrons in Yb are electronically isolated. Thus, the combination of bulk magnetization, theory and magnetic X-ray circular dichroism measurements strongly support $Yb_{14}MnSb_{11}$ as a candidate half-metallic ferromagnet.

IV. ACKNOWLEDGEMENTS

We thank R.N. Shelton for use of the magnetometer and P. Klavins for technical assistance. This research is funded by NSF DMR-9803074 and by Campus Laboratory Collaborations Program of the University of California.

1 G. A. Prinz, Science **282**, 1660 (1998).

2 R. A. de Groot, F. M. Mueller, P. G. van Engen, *et al*., Physical Review Letters **50**, 2024 (1983).

3 V. Y. Irkhin and M. I. Katsnel'son, Uspekhi Fizicheskii Nauk **164**, 705 (1994).

4 R. Weht and W. E. Pickett, Physical Review B **60**, 13006 (1999).

5 R. A. de Groot and K. H. J. Buschow, Journal of Magnetism and Magnetic Materials **54-57**, 1377 (1986).

6 E. Kulatov and I. I. Mazin, Journal of Physics: Condensed Matter **2**, 343 (1990).

7 J. S. Moodera and D. M. Mootoo, Journal of Applied Physics **76**, 6101 (1994).

8 W. E. Pickett and D. J. Singh, Physical Review B **53**, 1146 (1996).

9 J. H. Park, E. Vescovo, H. J. Kim, *et al*., Nature **392**, 794 (1998).

10 T. Kise, T. Ogasawara, M. Ashida, *et al*., Physical Review B **85**, 1986 (2000).

11 K.-I. Kobayashi, T. Kimura, H. Sawada, *et al*., Nature **395**, 677 (1998).

12 Y. Ji, G. J. Strijkers, F. Y. Yang, *et al*., Physical Review Letters **86**, 5585 (2001).

13 S. P. Lewis, P. B. Allen, and T. Sasaki, Physical Review B **55**, 10253 (1997).

14 N. E. Brener, J. M. Tyler, J. Callaway, *et al*., Physical Review B **61**, 16582 (2000).

15 K. Schwarz, Journal of Physics F **16**, L211 (1986).

16 D. Sánchez-Portal, R. M. Martin, S. M. Kauzlarich, *et al*., Physical Review B (2001).

17 S. L. Brock, L. J. Weston, M. M. Olmstead, *et al*., Journal of Solid State Chemistry **107**, 513 (1993).

18 J. Y. Chan, S. M. Kauzlarich, P. Klavins, *et al*., Chemistry of Materials **9**, 3132 (1997).

19 J. Y. Chan, M. M. Olmstead, S. M. Kauzlarich, *et al*., Chemistry of Materials **10**, 3583 (1997).

20 J. Y. Chan, M. E. Wang, A. Rehr, *et al*., Chemistry of Materials. **9**, 2131 (1997).

21 J. Y. Chan, S. M. Kauzlarich, P. Klavins, *et al*., Physical Review B **57**, 8103 (1998).

22 G. Cordier, H. Schäfer, and M. Stelter, Zeitschrift fur Anorganische und Allgemeine Chemie **519**, 183 (1984).

23 J. Del Castillo, D. J. Webb, S. M. Kauzlarich, *et al*., Physical Review B **47**, 4849 (1993).

24 I. R. Fisher, T. A. Wiener, S. L. Bud'ko, *et al*., Physical Review B **59**, 13829 (1999).

25 I. R. Fisher, S. L. Bud'ko, C. Song, *et al*., Physical Review Letters **85**, 1120 (2000).

26 R. F. Gallup, C. Y. Fong, and S. M. Kauzlarich, Inorganic Chemistry **31**, 115 (1992).

27 S. M. Kauzlarich, T. Y. Kuromoto, and M. M. Olmstead, Journal of the American Chemical Society **111**, 8041 (1989).

28 S. M. Kauzlarich and T. Y. Kuromoto, Croatica Chemica Acta **64**, 343 (1991).

29 S. M. Kauzlarich, M. M. Thomas, D. A. Odink, *et al*., Journal of the American Chemical Society **113**, 7205 (1991).

30 S. M. Kauzlarich, in *Chemistry, Structure, and Bonding of Zintl Phases and Ions*, edited by S. M. Kauzlarich (VCH Publishers, Inc., New York, 1996), p. 245.

31 T. Y. Kuromoto, S. M. Kauzlarich, and D. J. Webb, Molecular Crystals and Liquid Crystals **181**, 349 (1989).

32 T. Y. Kuromoto, S. M. Kauzlarich, and D. J. Webb, Chemistry of Materials **4**, 435 (1992).

33 A. C. Payne, M. M. Olmstead, S. M. Kauzlarich, *et al*., Chemistry of Materials **13**, 1398 (2001).

34 A. Rehr and S. M. Kauzlarich, Journal of Alloys and Compounds **207**, 424 (1994).

35 A. Rehr, T. Y. Kuromoto, S. M. Kauzlarich, *et al*., Chemistry of Materials **6**, 93 (1994).

36 D. P. Siemens, J. Del Castillo, W. Potter, *et al*., Solid State Communications **84**, 1029 (1992).

37 D. J. Webb, T. Y. Kuromoto, and S. M. Kauzlarich, Journal of Magnetism and Magnetic Materialsm **98**, 71 (1991).

38 D. J. Webb, T. Y. Kuromoto, and S. M. Kauzlarich, Journal of Applied Physics **69**, 4825 (1991).

39 D. J. Webb, R. Cohen, P. Klavins, *et al*., Journal of Applied Physics **83**, 7192 (1998).

40 D. M. Young, C. C. Torardi, M. M. Olmstead, *et al*., Chemistry of Materials **7**, 93 (1995).

41 P. C. Canfield and Z. Fisk, Philosophical Magazine B **65**, 1117 (1992).

42 J. G. Tobin, G. D. Waddill, and D. P. Pappas, Physical Review Letters **68**, 3642 (1992).

43 J. G. Tobin, G. D. Waddill, A. F. Jankowski, *et al*., Physical Review B **52**, 6530 (1995).

44 A. T. Young, V. Martynov, and H. A. Padmore, Journal of Electron Spectroscopy and Related Phenomena **101-103**, 885 (1999).

45 V. A. Formichev, S. A. Gribovskii, and T. M. Zimkina, Soviet Physics, Solid State **15**, 1880 (1974).

46 G. van der Laan and B. T. Thole, Physical Review B **43**, 13401 (1991).

47 P. Carra, B. T. Thole, M. Altarelli, *et al*., Physical Review Letters **70**, 694 (1993).

48 B. T. Thole, P. Carra, F. Sette, *et al*., Physical Review Letters **68**, 1943 (1992).

49 J. Y. Chan, S. M. Kauzlarich, P. Klavins, *et al*., Physical Review B **61**, 459 (2000).

50 C. Kittel, (John Wiley and Sons, Inc., New York, 1996), p. 627.

51 O. Toulemonde, F. Studer, A. Llobet, *et al*., Journal of Magnetism and Magnetic Materials **190**, 307 (1998).
52 A. Kimura, S. Suga, T. Shishidou, *et al*., Physical Review B **56**, 6021 (1997).
53 I. Galanakis, S. Ostanin, M. Alouani, *et al*., Physical Review B **61**, 4093 (2000).

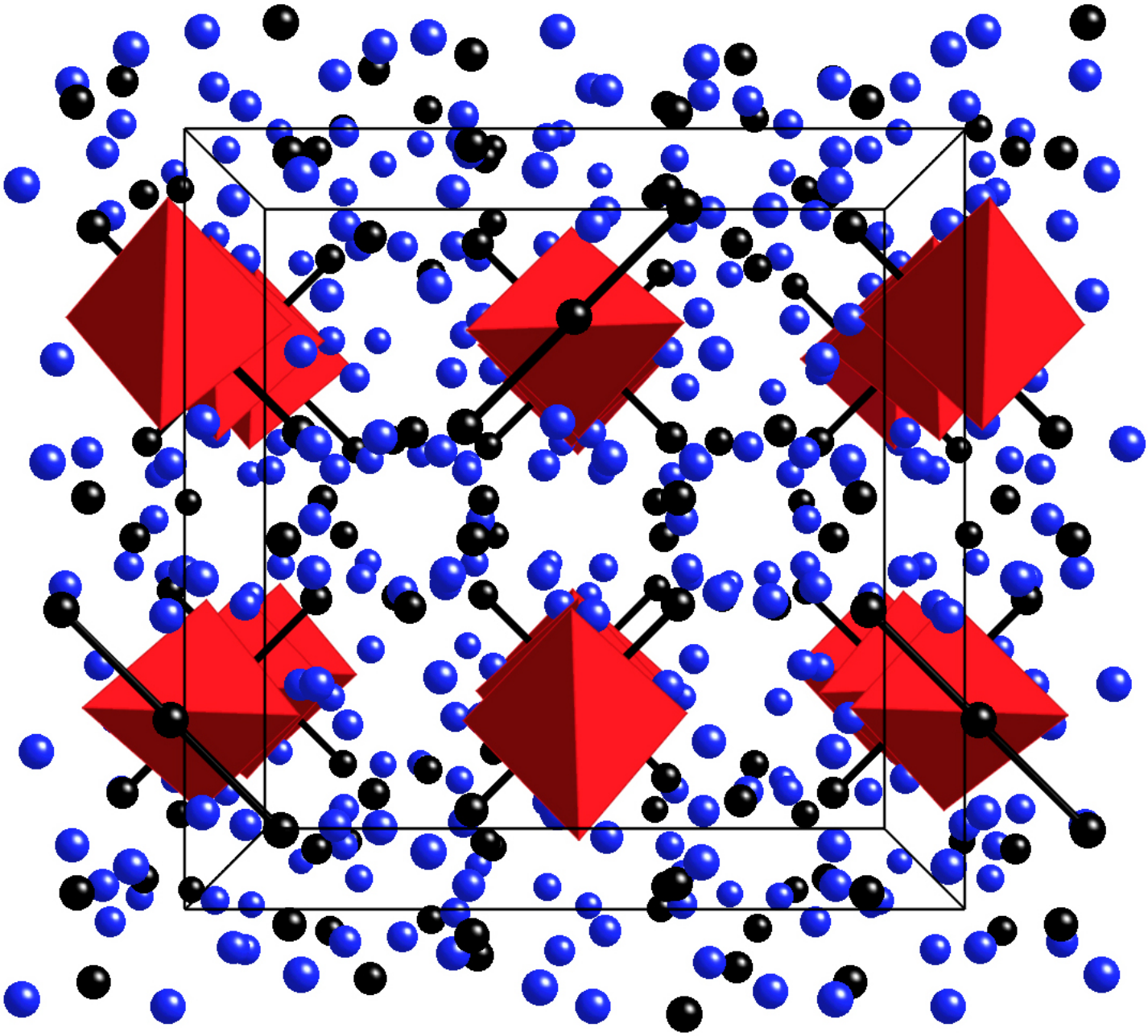

Fig. 1. Perspective view down the *c*-axis of the crystal structure of $Yb_{14}MnSb_{11}$. The $MnSb_4$ tetrahedra are shown in red and alternate with the Sb_3 linear units shown in black. The isolated Sb atoms are also shown in black, and the Yb atoms are shown in blue.

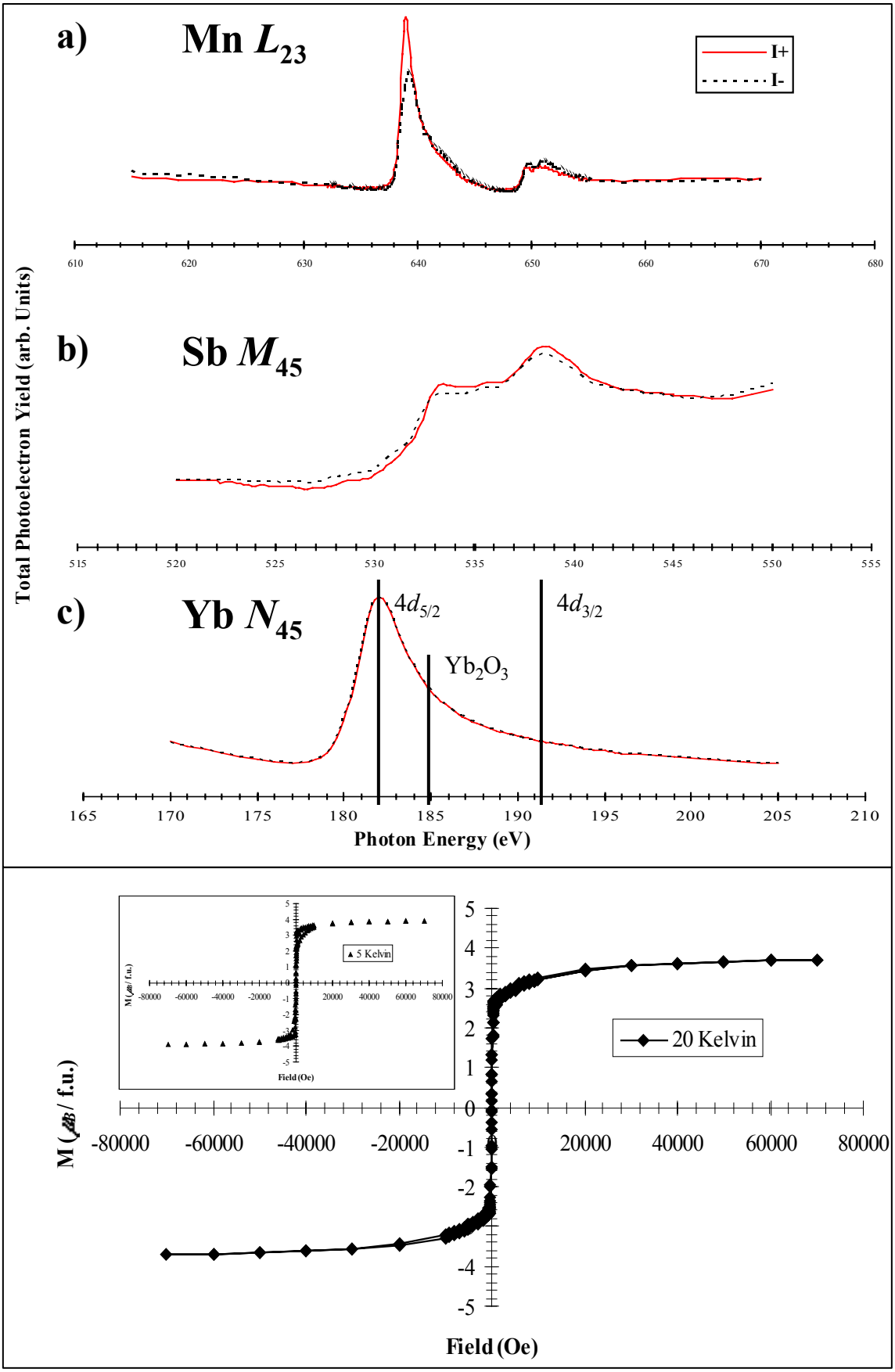

Fig. 2. The raw absorption spectra for a) Mn L_{23}, b) SbM_{45}, and c) Yb N_{45} are shown on top with the *M(H)* data at 20K and 5K (inset) shown on the bottom.

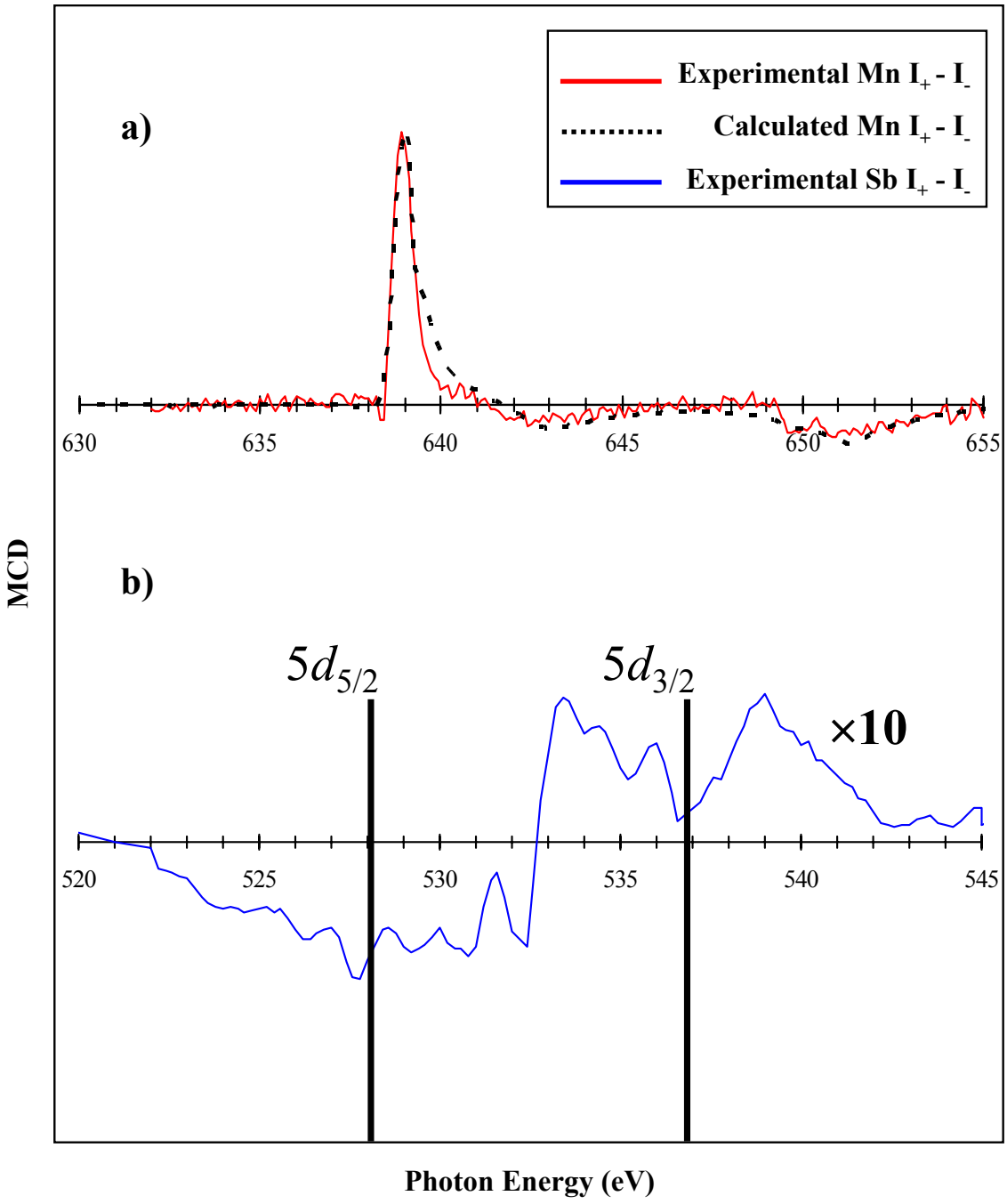

Fig 3. MCD spectra for the a) experimental and calculated Mn L_{23} denoted by a solid red line and a dashed black line respectively, and b) experimental Sb M_{45} denoted by a solid blue line.